PNAS RESEARCH ARTICLE | CELL BIOLOGY OPEN ACCESS

Reprogramming by drug-like molecules leads to regeneration of cochlear hair cell–like cells in adult mice

Yi-Zhou Quan[a,b,c,1], Wei Wei[a,b,c,d,1], Volkan Ergin[a,b,c,1], Arun Prabhu Rameshbabu[a,b,c], Mingqian Huang[a,b,c], Chunjie Tian[a,b,c], Srinivas Vinod Saladi[e,f], Artur A. Indzhykulian[a,b,c], and Zheng-Yi Chen[a,b,c,2]

Edited by Trudi Schüpbach, Princeton University, Princeton, NJ; received September 8, 2022; accepted March 2, 2023

Strategies to overcome irreversible cochlear hair cell (HC) damage and loss in mammals are of vital importance to hearing recovery in patients with permanent hearing loss. In mature mammalian cochlea, co-activation of *Myc* and *Notch1* reprograms supporting cells (SC) and promotes HC regeneration. Understanding of the underlying mechanisms may aid the development of a clinically relevant approach to achieve HC regeneration in the nontransgenic mature cochlea. By single-cell RNAseq, we show that MYC/NICD "rejuvenates" the adult mouse cochlea by activating multiple pathways including Wnt and cyclase activator of cyclic AMP (cAMP), whose blockade suppresses HC-like cell regeneration despite *Myc*/*Notch* activation. We screened and identified a combination (the cocktail) of drug-like molecules composing of small molecules and small interfering RNAs to activate the pathways of *Myc, Notch1, Wnt* and *cAMP*. We show that the cocktail effectively replaces *Myc* and *Notch1* transgenes and reprograms fully mature wild-type (WT) SCs for HC-like cells regeneration in vitro. Finally, we demonstrate the cocktail is capable of reprogramming adult cochlea for HC-like cells regeneration in WT mice with HC loss in vivo. Our study identifies a strategy by a clinically relevant approach to reprogram mature inner ear for HC-like cells regeneration, laying the foundation for hearing restoration by HC regeneration.

adult mouse cochlea | hair cell regeneration | reprogramming | RNAseq | small moleules and siRNA

Hearing loss affects one in 500 newborns and half of the population over 70 y old worldwide (1, 2). Despite being one of the most common forms of human sensory deficits, there is currently no pharmacological therapy for hearing loss. The mammalian inner ear detects sound through the function of hair cells (HCs), the sensory cells that convert sound signals into electrical impulses (3). HC loss is considered the major cause of hearing loss (4, 5). However, the mature mammalian inner ear does not have the capacity to spontaneously repair or regenerate HCs after HC damage or loss, leading to permanent hearing loss.

To use HC regeneration for hearing restoration, different strategies have been pursued. Various evidence suggests that HC regeneration in mammals is possible. Spontaneous HC regeneration occurs in lower vertebrates including birds and fish that leads to functional recovery (2, 6, 7). Embryonic and neonatal mouse cochlea also retains the capacity to regenerate HCs by enhancing expression of specific genes essential for HC development (8–10). Activating Sonic Hedgehog signaling resulted in cell cycle re-entry and production of HC in the neonatal cochlear sensory epithelium (SE) (11, 12). The ERBB2 pathway was shown to promote supporting cell (SC) proliferation with increased MYO7A$^+$ cells in neonatal mice (13). However, the capacity to generate HCs decreases rapidly 2 wk after birth, even with the manipulation of multiple signal pathways (9). Though early studies provided evidence that manipulating signal pathways had a similar effect in the adult mammalian cochlea (14–17), compared to the neonatal stage, the efficiency to regenerate HCs in the adult mouse cochlea has been exceedingly low.

To achieve HC regeneration in the adult cochlea, we hypothesized a two-phase process could be sufficient: 1) To reprogram mature cochlear SCs to regain the properties of their young biological selves; 2) To activate an HC fate-determining factor (*Atoh1*) in the reprogrammed adult SCs for HC regeneration. We have shown that, by transient co-activation of *Myc* and *NICD* (*Notch1 intracellular domain*), the adult mouse cochlea can be successfully reprogrammed to a relatively younger stage and regain progenitor capacity, with the regeneration of HC-like cells following *Atoh1* overexpression in vitro and in vivo (18). In the study, reprogramming and HC regeneration were achieved through the manipulation of the transgenes of *Myc* and *Notch1* in a transgenic mouse model. However, it remains a major challenge to develop a similar strategy for HC regeneration in the wild-type (WT) mature inner ear that is potentially clinically applicable.

Significance

Hearing loss affects millions of people without a single FDA-approved drug for treatment. The loss of the inner ear sensory cells, the hair cells, is considered one of the most common causes of hearing loss that is generally permanent. Such loss cannot be compensated by the terminally differentiated supporting cells, which do not readily transdifferentiate into new hair cells in adult mouse cochleae. Using single-cell RNAseq, advanced imaging, electrophysiology, and lineage tracing, Quan et al. identified a combination (the cocktail) of drug-like molecules composed of small molecules and siRNAs that effectively reprograms fully mature wild-type supporting cells for hair cell-like cell regeneration in a mouse model with hair cell loss, representing a step forward for hearing restoration by HC regeneration.

Competing interest statement: The authors have organizational affiliations to disclose, Z.-Y.C. is a co-founder and a SAB member of Salubritas Therapeutics, which is developing treatments for hearing loss including genome editing, inner ear regeneration, novel delivery, and gene therapy. Z.-Y.C. has ownership of over 5% equity of Salubritas Therapeutics. Y.-Z.Q. and Z.-Y.C. are co-inventors on a patent application that has been filed based on the study by MEE. A patent application on the combination of small molecules/siRNAs in hair cell regeneration has been filed.

This article is a PNAS Direct Submission.

[1]Y.-Z.Q., W.W., and V.E. contributed equally to this work.

[2]To whom correspondence may be addressed. Email: Zheng-Yi_Chen@meei.harvard.edu.

This article contains supporting information online at https://www.pnas.org/lookup/suppl/doi:10.1073/pnas.2215253120/-/DCSupplemental.

Published April 17, 2023.

To identify the molecules that can reprogram mature cochlear SCs, we performed single-cell RNAseq and uncovered the pathways and their target genes underlying MYC/NICD mediated reprogramming. We screened small chemical compounds and small interfering RNAs (siRNA) to efficiently target downstream pathways and genes. Using a cocktail composed of small molecules and siRNAs, we demonstrate that *Myc* and *Notch1* genes can be effectively replaced to reprogram terminally differentiated mature cochlear epithelial cells, including SOX2$^+$ SCs, which regain progenitor properties and efficiently transdifferentiate into HC-like cells in the adult inner ear in vitro. Significantly, the strategy is shown to sufficiently reprogram the SE and regenerate HC-like cells in the WT adult mouse inner ear following HC loss in vivo. Our data support that regeneration of cochlear HC-like cells can be achieved in adult mice using a drug-like approach with clinical implications.

Results

The Synergistic Reprogramming Effect by MYC/Valproic acid (VPA) and siRNAs/VPA. Mature cochlear epithelial cells lack the capacity to respond to the HC induction signals including *Atoh1* overexpression or *Rb* inhibition to regenerate HCs (9, 19). We have developed a strategy to regenerate HC in the mature cochlea by reprogramming through transient activation of MYC/NICD followed by HC induction by Ad.*Atoh1* infection in a transgenic mouse model (rtTA/tet-Myc/tet-NICD) (18) (*SI Appendix*, Fig. S1)

To advance our approach toward potential clinical application, it is necessary to reprogram SCs in the WT non-transgenic mature mammalian inner ear by a clinically relevant method that is sufficient to replace the functions of transgenes *Myc* and *Notch1.*

VPA, a histone deacetylase (HDAC) inhibitor, is a well-known Notch activator in multiple organs (20, 21) and is capable of expanding the sensory progenitors in neonatal cochleae (22). We treated cultured adult WT cochlea with VPA and used qPCR to confirm VPA treatment upregulated *Notch1* significantly (*SI Appendix*, Fig. S2*A*). We hypothesized that VPA/MYC may synergistically reprogram the mature mouse cochlea for HC regeneration. To test the hypothesis, we bred rtTA/tet-*MYC* mice with Atoh1-GFP reporter mice to create a rtTA/tet-*MYC*/Atoh1-GFP model. We tested our hypothesis using an adult mouse cochlea culture system, in which a majority of SOX2$^+$ SC survived, whereas all OHCs and a majority of IHCs were lost rapidly in culture (18, 23). The cultured adult rtTA/tet-*MYC*/Atoh1-GFP cochleae were treated by doxycycline (Dox) to activate *Myc* and VPA for 4 d followed by infection of ad.*Atoh1* in culture (Fig. 1*A*). 14 d after Ad.*Atoh1* infection, significantly more HC-like cells (MYO7A$^+$/GFP$^+$) were generated (Fig. 1 *C1*–*C3* and *D*). In contrast, in cultured adult rtTA/tet-*MYC*/Atoh1-GFP cochlea infected with ad.*Atoh1* alone, sporadic-infected cells (GFP$^+$) became HC-like cells (Fig. 1 *B1*–*B3* and *D*), despite a similar infection rate (shown by GFP$^+$) by ad.*Atoh1* in Dox-treated and vehicle-treated control groups (Fig. 1*E*). The regenerated HC-like cells have the characteristics of the neonatal and immature HC. By scanning electron microscopy (SEM), we identified regenerated HC-like cells with kinocilia, a HC structure that only presents in the neonatal cochlear HCs (24). Indeed, regenerated immature HC-like cells with and without kinocilia were detected (Fig. 1 *F*–*I*) in the VPA/Dox/ad.*Atoh1*-treated rtTA/tet-*MYC* cochleae, an indication of new HC-like cells. Some regenerated HC-like cells were also labeled with an SC marker SOX2 (Fig. 1 *J*–*M*, arrows), resembling the neonatal HCs in the normal development of the embryonic mouse cochlea, supporting the SC origin of the regenerated HC-like cells. Importantly, a similar number of HC-like cells were regenerated in the SE between the VPA/Dox-treated rtTA/tet-*Myc* (16 ± 2.38, mean ± SD, per 100 μm) and Dox-treated rtTA/tet-*Myc*/tet-*NICD* adult cochleae (24.3 ± 4.08, mean ± SD, per 100 μm) (Fig. 1*E* vs. *SI Appendix*, Fig. S1*C*), supporting that VPA/MYC could synergistically reprogram adult cochlea for HC-like cell regeneration.

Unlike VPA that robustly activates *Notch*, there is no potent small molecule activator of *Myc.* As an alternative, we sought to activate *Myc* by suppressing *Myc* suppressors using siRNAs. We tested the siRNAs for the *Myc* suppressors *Fir* (siF) and *Mxi1* (siM) (25, 26) in the cultured adult cochlea. The siRNAs for *Fir* and *Mxi1* suppressed the respective gene and when combined, they resulted in moderate *Myc* activation (*SI Appendix*, Fig. S2*A*). To evaluate the effect of the siRNAs in HC regeneration, we combined VPA with the two siRNAs (siFsiM) and treated cultured WT adult cochlea for 4 d followed by the administration of Ad.*Atoh1-mCherry* for 14 d (*SI Appendix*, Fig. S2*B*). New MYO7A$^+$/Atoh1-mCherry$^+$ HC-like cells were detected in the treated adult mouse cochlea (*SI Appendix*, Fig. S2 *C* and *D*). However, compared to HC regeneration in the Dox-treated rtTA/tet-*Myc*/tet-NICD or VPA-treated rtTA/tet-*Myc* models, the regeneration efficiency by VPA/siRNAs is significantly reduced (*SI Appendix*, Figs. S2*D* vs. *SI Appendix*, Fig. S1*C*, *SI Appendix*, Fig. S2*D* vs. Fig. 1*D*). We conclude that the *Fir/Mxi1* siRNAs treatment activates MYC that leads to HC-like cell regeneration at a reduced efficiency than *Myc* transgene activation. To improve HC regeneration efficiency in WT non-transgenic mature mammalian cochlea, further manipulations will be necessary.

Single-Cell RNAseq Reveals Diverse Cellular Response to *Myc/NICD*-Mediated Reprogramming. As MYC/NICD potently reprograms adult cochlea for efficient HC regeneration, uncovering the underlying pathways should aid our understanding of the reprogramming mechanisms and importantly provide us with the knowledge to develop an HC regeneration strategy that may be clinically relevant. We used an adult cochlea explant culture system (18) and single-cell RNAseq to study global gene expression profiles of the transgenic mouse model, rtTa/tet-*Myc/-tet-NICD,* in response to Dox-induced MYC/NICD co-activation mediated reprogramming. We have shown that a 4-d treatment by Dox in cultured adult rtTa/tet-*Myc/-tet-NICD* cochleae was sufficient to reprogram adult SCs for efficient HC regeneration (18). We thus treated cultured adult rtTa/tet-*Myc/-tet-NICD* cochleae with Dox for 4 d before the harvest to create cDNA libraries for NGS processing (Fig. 2*A* and *Methods*). By CellRanger pipeline, we acquired single-cell transcriptomes in a total of 512 cells from control samples and 1,883 cells from Dox-treated samples (*SI Appendix*, Fig. S3*A*). Following filtering (*SI Appendix*, Fig. S3*B*) by the Seurat v.3.2 (27), the scRNA-seq data were clustered by the principal component which identified nine distinct clusters. Based on the previous single-cell RNAseq studies in the cochlea (28–32), cell clusters were assigned: interdental cells (IdC), Claudius cells/outer sulcus cells (CCOS), Reissner's membrane cells (RMC), Deiter's cells (DC), Kolliker's organ cells (KO), Hensen's cells (HeC), unclassified-SCs (uSC), macrophage-like cells (MLC), and HC (Fig. 2*C*). After Dox treatment, *Myc* and *Notch1* were upregulated compared to the untreated control group (Fig. 2 *D* and *E*). The cell identities of each cluster were associated with known cell type marker gene expression (*SI Appendix*, Fig. S4*A* and Table S1), including *Galm*, *Nfix*, *Epcam* for IdC; *Cp*, *Col3a1*, *Fstl1* for CCOS; *Vmo1*, *Meis2*, *Fut9* for RMC; *Bace2*, *Caecam16*, *Car14* for DC; *Epyc*, *Slc39a8*, *Lum* for KO; *Plp1*, *Pmp22*, *Sostdc1* for HeC; *Cx3cr1*, *Emilin2*, *Fcgr1* for MLC; and *Pvalb*, *Atp8a2*, *Nefl* for HC (*SI Appendix*, Fig. S4 *B* and *C*). For the cluster uSC, genes such as *Gdf15*, *Ciart*,

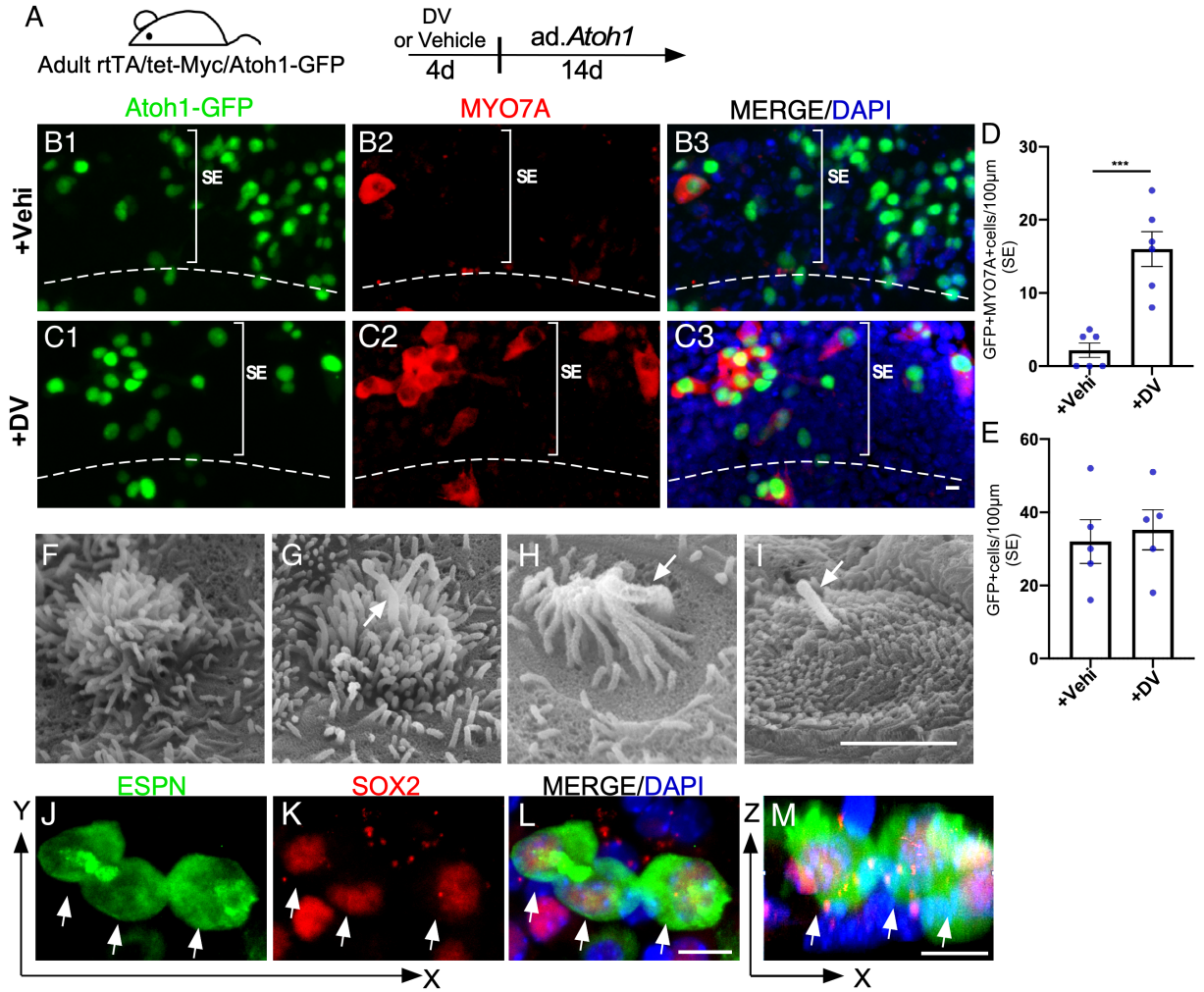

Fig. 1. VPA/MYC synergistically reprogram adult SCs for HC-like cell regeneration. (*A*) A schematic diagram illustrating the experimental procedure of the cultured adult cochleae treated transiently by Dox to induce *Myc* and VPA to activate *NICD* (DV) and HC-like cell induction by Ad.*Atoh1*. (*B* and *C*) Vehicle (sterile water)/Ad.*Atoh1* or Dox/VPA/Ad.*Atoh1*-treated adult (P30) rtTA/tet-*Myc*/Atoh1-GFP mice cochleae were labelled with MYO7A/GFP. Regenerated HC-like cells (MYO7A$^+$/Atoh1-GFP$^+$) were seen in the DV-treated group and occasional HCs were seen in the control sample. GFP$^+$ cells were Ad.*Atoh1* infected. (*D* and *E*) Quantification and comparison of regenerated HC-like cells and GFP$^+$ cells in the apical turn of the cultured cochleae between Dox/VPA/Ad.*Atoh1*-treated and vehicle/Ad.*Atoh1*-treated groups. Significantly more HC-like cells were seen in the DV-treated than in control samples (*D*) and a similar number of GFP$^+$ cells, i.e., the Ad.*Atoh1*-infected cells, were seen in the two groups (*E*). ***$P < 0.001$, two-tailed unpaired Student's *t* test. Error bar, mean ± SEM, n = 5. (*F–I*) Images of scanning electron microscopy (SEM) showing immature stereocilia from regenerated HC-like cells in rtTA/tet-*Myc*/Atoh1-GFP cochlea treated with Dox/VPA and Ad.*Atoh1* in vitro. Arrows point to kinocilia. (*J–M*) Regenerated HC-like cells (ESPN$^+$) co-labeled with SOX2 (arrows) were seen in a cultured adult (P30) rtTA/tet-*Myc* mouse cochlea treated with Dox/VPA/Ad.*Atoh1*. Arrows point to the SOX2$^+$/ESPN$^+$ double-positive HC-like cells. SE: sensory epithelial region. (Scale bar in *F–I*: 2 μm; *J–M*: 10 μm.)

Hspa1a could not be assigned to an existing known cluster within the cochlea, indicating the cluster may contain the cells whose expression profiles were drastically altered by culturing conditions and/or Dox treatment. We did not detect certain cochlear cell type clusters such as pillar cells and stria vascularis cells. In summary, we profiled the transcriptomes of most cell types in the cultured adult cochlea with and without *Myc/Nocth1* activation.

Identification of Reprogramming Pathways Mediated by *Myc/Notch1* Co-activation. To characterize the molecular signature during reprogramming, we performed differential gene expression analysis and pathway enrichment analysis (*SI Appendix*, Fig. S5). First, we observed almost no overlap of differentially expressed genes between the two groups (*SI Appendix*, Fig. S5*A* and Table S2), supporting that co-activation of *Notch1* and *Myc* profoundly affects overall gene expression of the cultured cochlea. By Gene Set Enrichment Analysis (33, 34), we identified genes prominently enriched under *Myc/Notch1* co-activation in the pathways including MYC targets and NOTCH signaling, E2F targets, G2M checkpoint, oxidative phosphorylation, and mTORC1 (*SI Appendix*, Fig. S5*B*). We visualized the genes from the top five Hallmark sets and found the IdCs cluster to have the most distinct expression profiles that were high in the Dox-treated compared to the control groups (*SI Appendix*, Fig. S5*C*), suggesting that the IdCs were more sensitive to MYC/NICD-mediated reprogramming than other cochlear cell types. Among the pathways highly activated in the IdCs included E2F targets and G2M, and both are involved in proliferation. We tested the hypothesis that the IdCs were more sensitive to MYC/NICD co-activation to proliferate by studying EdU incorporation in the cultured adult rtTA/tet-MYC/tet-NICD cochlea treated with Dox. In the limbus region (the IdC cluster), a large number of EdU$^+$ cells were observed compared to other cell types such as the SE (IdC region v.s. SE region; *SI Appendix*, Fig. S5 *D* and *E*), supporting that the IdC undergo more robust reprogramming in response to MYC/NICD. In control cultured rtTA/tet-MYC/tet-NICD cochlea without Myc/Notch1 activation, virtually no EdU-labeled cells were detected (*SI Appendix*, Fig. S5 *D* and *E*).

In addition to a greater proliferation potential, the IdCs have the highest regeneration potential among the cochlear cell types in vitro (*SI Appendix*, Fig. S1 *B3* and *D*) and in vivo (18),

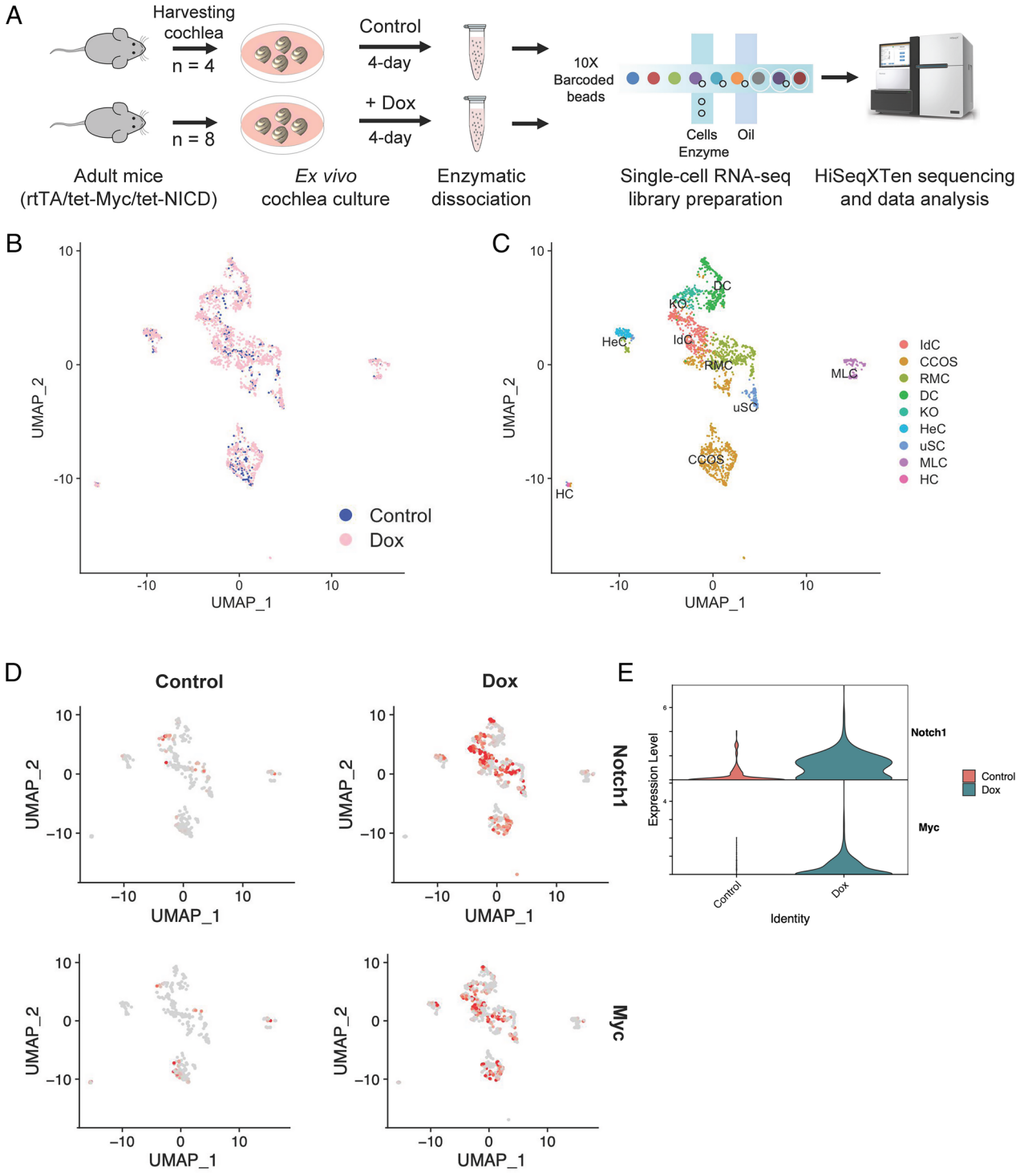

Fig. 2. Single-cell RNA sequencing identified putative cell types across the sensory epithelium from adult mouse cochlear explant culture. (*A*) Schematic diagram depicting the experimental setup for collection and processing of cochlear explants for the 10× Genomics Chromium Single-Cell 3′ Gene Expression workflow. (*B*) UMAP plot showing the putative clusters from the integrated analysis of control and Dox groups. (*C*) UMAP plot of 2,395 cells displaying each cell colored according to putative cluster assignment. (*D*) UMAPs colored by the normalized log-transformed expression of *Notch1* and *Myc*, showing Dox-induced transgene expression. The color key from gray to red indicates relative expression levels from low to high. (*E*) Violin plots illustrating normalized and Log-transformed expression profiles of *Notch1* and *Myc* transgenes between control and Dox-induced cochleae.

suggesting that the IdCs responded to reprogramming more efficiently, and as the consequence transdifferentiated to HC-like cells more readily in the presence of *Atoh1*. To further study the IdC clusters in programming based on scRNAseq, we selected the IdC clusters for subclustering (Fig. 3*A*). We performed pseudotime trajectory analysis using Monocle3 (35, 36) to reveal gene expression kinetics following Dox treatment that induced reprogramming. Based on the trajectory, the cells were then ordered in pseudotime by defining a starting node being the IdC control cells without reprogramming (Fig. 3*B*), and an ending node represented by the reprogrammed IdC Dox cells (Fig. 3*B*). The pseudotime trajectory captured the reprogramming process by four distinct regulatory modules with the genes (*SI Appendix*, Table S3) that co-expressed across individual cells, and each module containing a set of co-regulated genes corresponds to a unique state during the transition from IdC_Control to IdC_Dox state (Fig. 3*C*).

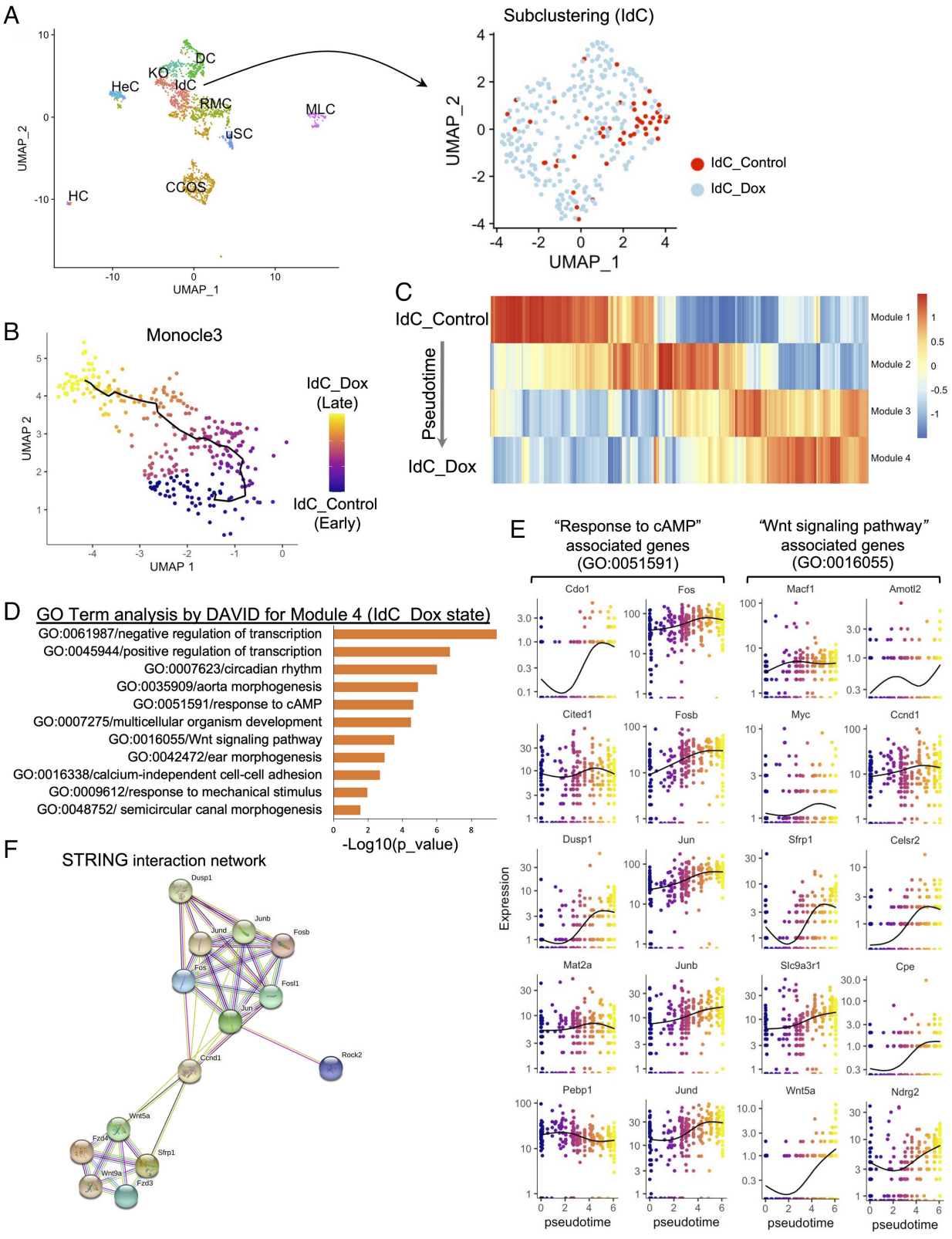

Fig. 3. Computational lineage modeling analysis for the reprogramming trajectory for the interdental cell (IdC) cluster. (*A*) Subclustering of the interdental cells (IdC) showing distinct accumulation of control (red) and the surrounding Dox-induced sample-derived IdC cells (light blue). (*B*) Construction of a pseudotime trajectory of the IdC subcluster from control to Dox-treated samples, with the black line showing the path of pseudotime, and UMAP plots are colored according to pseudotime. (*C*) Expression changes of the co-regulated genes within each module generated by Monocle3 analysis. The modules are consisted of genes clustered according to the correlation of expression levels. (*D*) Gene ontology analysis of Module 4 by DAVID using the genes whose expression changed significantly over pseudotime. The GO terms with p value less than 0.05 were considered significantly enriched by the query genes. (*E*) Kinetic plots showing the relative expression profiles of ten representative genes associated with Response to cAMP or Wnt Signaling Pathway over the pseudotime. (*F*) A functional interaction network of the key genes from the Response to cAMP and Wnt signaling pathways. The nodes represent proteins, and the colored lines represent interactions between proteins. Presence of the more lines denotes a greater degree of connection.

We then performed pathway analysis by The Database for Annotation, Visualization and Integrated Discovery (DAVID) on the list of co-regulated genes in each of the four modules revealed by Monocle3 (35, 36). DAVID identified Module 1 as the baseline state of unreprogrammed IdCs control with the prominent expression of chromatin silencing and epigenetic regulation genes (*SI Appendix*, Fig. S6*A*). In Module 2, the genes representing an early transition state were mostly cytoskeletal and post-translational modification regulatory genes such as kinases, nucleosome and ubiquitin-conjugation enzymes (*SI Appendix*, Fig. S6*B*). In Module 3 of a late transition state, the genes of extracellular matrix or cell-cell adhesion-related genes were enriched (*SI Appendix*, Fig. S6*C*). Lastly, in Module 4 representing the Dox-induced reprogrammed state, co-regulated genes were enriched for transcriptional regulation, morphogenesis, development, and mechanosensing (Fig. 3*D*), supporting the gene classes contributing to initiation and progression of reprogramming, and/or differentiation capacity of the reprogrammed IdC cells by MYC/NOTCH co-activation.

Wnt and cyclase activator of cyclic AMP (cAMP) Are Downstream of MYC/NICD-Mediated Reprogramming and Are Necessary for HC Regeneration. In addition to the identification of the pathways in reprogramming, our main goal is to identify possible small molecules that target the pathways for reprogramming. In Module 4, while DAVID showed highly represented Gene Ontology (GO) classes, the Wnt and cAMP-induced signaling pathways could be targeted by small molecules (Fig. 3*D*). We thus focused on Wnt and cAMP pathways that may play significant roles in the acquisition and establishment of the reprogrammed-state of the IdCs by Dox induction. To better evaluate the relationship of Wnt and cAMP pathway genes in the IdC clusters during reprogramming, we plotted gene expression profiles of selected Wnt and cAMP pathways genes from Module 4 as a function of pseudotime (Fig. 3*E*). Ten representative genes for the Wnt pathway or cAMP-response pathway showed an overall gradual increase in their expression levels during transition from un-reprogrammed control to the reprogrammed state by Dox induction, supporting that these pathways are part of reprogramming process. Using the STRING tool (37), we constructed a protein-to-protein interactive network composed of Wnt- and cAMP-related genes connected by *Ccnd1* (Fig. 3*F*). Overall, we found that IdCs are highly sensitive to MYC/NICD induced reprogramming, which may underlie their heightened potential to transdifferentiate to HC-like cell.

The identification of Wnt and cAMP upon MYC/NICD activation suggests the important roles for each pathway in HC regeneration in mature cochlea. To confirm the results from the scRNA-seq study, we measured the expression of selected Wnt and cAMP pathway genes by qRT-PCR in cultured adult rtTA/tet-*Myc*/tet-NICD cochlea after Dox treatment and detected upregulation of Wnt and cAMP pathways genes in the Dox treatment group (*SI Appendix*, Fig. S7). To determine if Wnt and/or cAMP is required for MYC/NICD-mediated reprogramming for HC regeneration, we activated MYC/NICD in cultured adult rtTA/tet-*Myc*/tet-NICD cochlea by Dox, in the presence of small molecule Wnt inhibitor IWP2, cAMP inhibitor BI (bithionol), or both IWP2+BI (38, 39), with the cochleae subsequently infected by Ad.*Atoh1-mCherry*. In control cochlea without Wnt or cAMP inhibitors, Dox-induced MYC/NICD reprogrammed adult cochlear cells in the SE and the limbus region responded to *Atoh1* and transdifferentiated to HC efficiently (*SI Appendix*, Fig. S7 *C–E*). In the cochlear groups treated with the Dox+IWP2, Dox+BI or Dox +IWP2+BI, HC regeneration was severely attenuated despite the presence of abundant Ad.*Atoh1-mCherry*-infected cells in the SE and the limbus region (*SI Appendix*, Fig. S7 *C–E*). The Bi/Iwp2 combination had a stronger inhibitory effect than BI or Iwp2 alone in the sensory epithelial region (*SI Appendix*, Fig. S7*E*). Taken together, we demonstrated that in the adult mouse cochlea, Wnt and cAMP pathways were activated by MYC/NICD activation, and both are necessary for reprogramming of adult cochlear cells and their transdifferentiation to HC in the sensory and non-sensory regions.

The necessity of Wnt and cAMP in MYC/NICD mediated HC regeneration suggests their activation could facilitate HC regeneration. To maximize the efficiency in HC regeneration, we combined VPA, siFIR, and siMxi1 (VsiFsiM) with a Wnt agonist LiCl(L) and a cAMP agonist Forsklin (FSK, F) to constitute a VLFsiFsiM "cocktail". We tested reprogramming by applying the cocktail to cultured adult WT cochleae and studied the activation of inner ear progenitor genes. qPCR showed upregulation of *Myc, Notch1* and progenitor genes including *Six1, Eya1* and *Gata3*, but not embryonic stem cell genes like *Nanog* and *Fut4* (*SI Appendix*, Fig. S8 *A* and *B*), mimicking the reprogramming effect of MYC/NICD in the transgenic mice (18).

Regeneration of HC-Like Cells by the Cocktail-Driven Reprogramming in WT Adult Mouse Cochlea In Vitro. To determine the potency of the VLFsiFsiM cocktail to reprogram adult WT cochlea for HC regeneration in vitro, we added the cocktail to cultured adult C57BL/6J mouse cochleae for 4 d followed by infection by Ad.*Atoh1.mCherry* for 14 d (Fig. 4*A*). Ad.*Atoh1.mCherry*-infected a similar number of SC in the cocktail-treated and untreated control cochleae shown by mCherry signal (Fig. 4 *A*, *B1*, *C1*, *D*, and *F*). In the cocktail-treated cochleae, we found numerous HC-like cells (POU4F3$^+$/MYO7A$^+$) regenerated in the adult cochlear SE and the limbus region (Fig. 4 *C*, *E*, and *G*). In contrast, in control adult cochlea without cocktail treatment, Ad.*Atoh1.mCherry* infection resulted few new HC-like cells (Fig. 4 *B*, *E*, and *G*). HC regeneration efficiency following the cocktail treatment was similar to that obtained using the transgenic mouse model (Fig. 4 *E* and *G* and *SI Appendix*, Fig. S1 *C* and *D*), which strongly supports potent reprogramming by the cocktail. We performed lineage tracing study to determine the origin of new HC-like cells, using the Sox2CreER-tdTomato (tdT) model in which tamoxifen exposure activates tdT permanently in the SOX2$^+$ SC. We found that after cocktail+Ad.*Atoh1* treatment, new HC-like cells were co-labeled with tdT (arrowheads, Fig. 4 *H–J*), demonstrating SC origin of regenerated HC-like cells.

To study if the new HC-like cells possess functional transduction channels, we performed FM1-43 uptake by regenerated HC-like cells 14 d after Ad.*Atoh1* infection. We added the cocktail to cultured adult Atoh1-GFP mouse cochleae, in which the Atoh1 enhancer drives expression of a nuclear GFP reporter, allowing the tracking of the cells with *Atoh1* expression. FM1-43 is a fluorescent dye that passes through functional transduction channels and is trapped by its charge with HCs. We observed FM1-43$^+$/Atoh1-GFP$^+$/MYO7A$^+$ triple positive HC-like cells in the cocktail-treated group, indicating the uptake of the dye by new HC-like cells (Fig. 4*K*). New HC-like cells are positive for developing HC markers including POU4F3 and PCP4 (*SI Appendix*, Figs. S9 *A–C* and S10). Interestingly, we found some Atoh1-GFP$^+$/MYO7A$^+$ and POU4F3$^+$/PCP4$^+$ HC-like cells in clusters with a sphere-like structures in the cocktail-treated group (Fig. 4*L* and *SI Appendix*, Fig. S9*C*), reminiscent of the spheres derived from inner ear stem cells, suggesting the reprogramming process may expand stem cells/progenitors from which subsequently transdifferentiated to HC-like cells. By SEM, we detected regenerated HC-like cells with immature stereocilia, and with or without kinocilia (*SI Appendix*, Fig. S9 *D1–D3*). We further used acetylated tubulin (Ac-TUBA4A) labeling to examine the presence

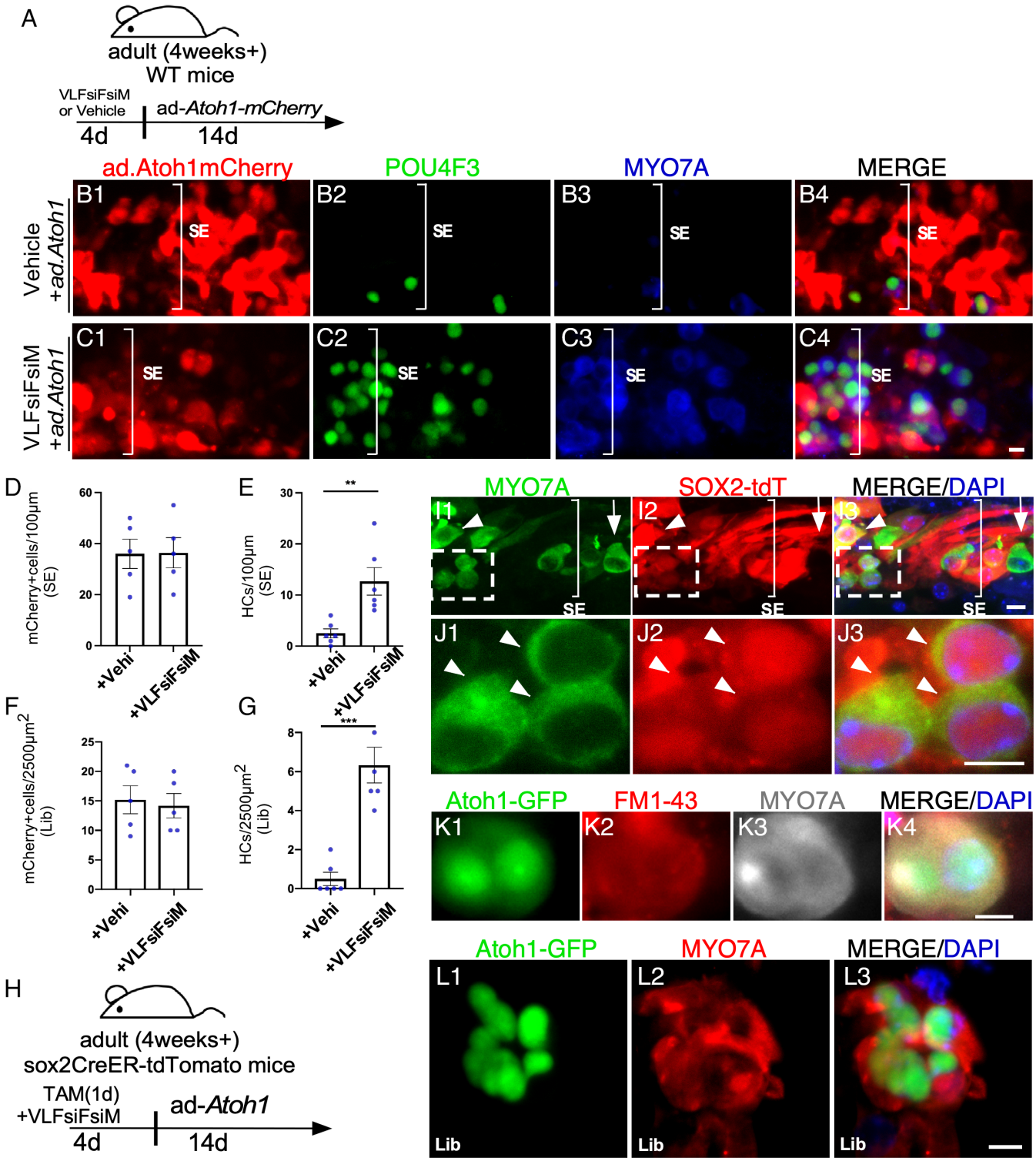

Fig. 4. A cocktail of siRNAs and small molecules to replace MYC/NICD in reprogramming for HC-like cell regeneration in adult cochlea in vitro. (*A*) A schematic diagram illustrating the experimental procedure of VLFsiFsiM/Ad.*Atoh1* induced HC-like cell regeneration. (*B* and *C*) The cocktail (VLFsiFsiM)/Ad.*Atoh1.mCherry* or vehicle/Ad.*Atoh1.mCherry* treated adult (P30) WT mouse cochlear samples were labeled with MYO7A (blue)/POU4F3 (green) in the sensory epithelial region. Numerous HC-like cells (POU4F3$^+$/MYO7A$^+$) were seen in the apex of the VLFsiFsiM/Ad.*Atoh1.mCherry*-treated cochlea. (*D*–*G*) Quantification and comparison of infected cells and regenerated HC-like cells in the apical turn of the cultured cochleae between VLFsiFsiM/Ad.*Atoh1.mCherry*-treated and vehicle/Ad.*Atoh1.mCherry*-treated groups. Significantly more HC-like cells were regenerated in the VLFsiFsiM/Ad.*Atoh1*-treated than vehicle/Ad.*Atoh1*-treated samples (*E* and *G*) in the sensory epithelial (SE) and the limbus (Lib) regions, respectively. The number of Ad.*Atoh1.mCherry*-infected cells between the two conditions was similar (*D* and *F*). (*H*) A schematic diagram illustrating the experimental procedure of lineage tracing for new HC-like cells after VLFsiFsiM/Ad.*Atoh1* treatment. (*I*) In the cultured Sox2CreER/tdT adult cochlea, Tamoxifen (Tamo) induced tdT in the SCs which transdifferentiated to HC-like cells by VLFsiFsiM/Ad.*Atoh1* treatment, shown by MYO7A$^+$/Sox2-tdT$^+$ labeling. The arrow indicates an existing HC, which was MYO7A$^+$/Sox2-tdT$^-$. The arrowhead indicates a regenerated HC-like cell, shown by MYO7A$^+$/Sox2-tdT$^+$ labeling. (*J*) Enlarge inset from *H* to show the lineage traced HC-like cells (MYO7A$^+$/Sox2-tdT$^+$) (arrowheads). (*K*) VLFsiFsiM/Ad.*Atoh1*-treated adult (P30) *Atoh1*-GFP mouse cochlear samples showed infected cells (GFP$^+$) that transdifferentiated to HC-like cell (MYO7A$^+$) and were able to take up FM1-43. (*L*) A cluster of HC-like cells (MYO7A$^+$) was seen in the VLFsiFsiM/Ad.*Atoh1*-treated adult cochlea. T, Tamo: 4-hydroxytamoxifen. V: VPA; L: LiCl; F: FSK; siF: siFIR; siM: siMxi1. SE: sensory epithelial region. Lib: Limbus Region. $^{**}P < 0.01$, $^{***}P < 0.001$, Student's *t* test. Error bar, mean ± SEM; N = 5 to 6 in each group. Source data are provided as a Source Data file. (Scale bars, 10 μm.)

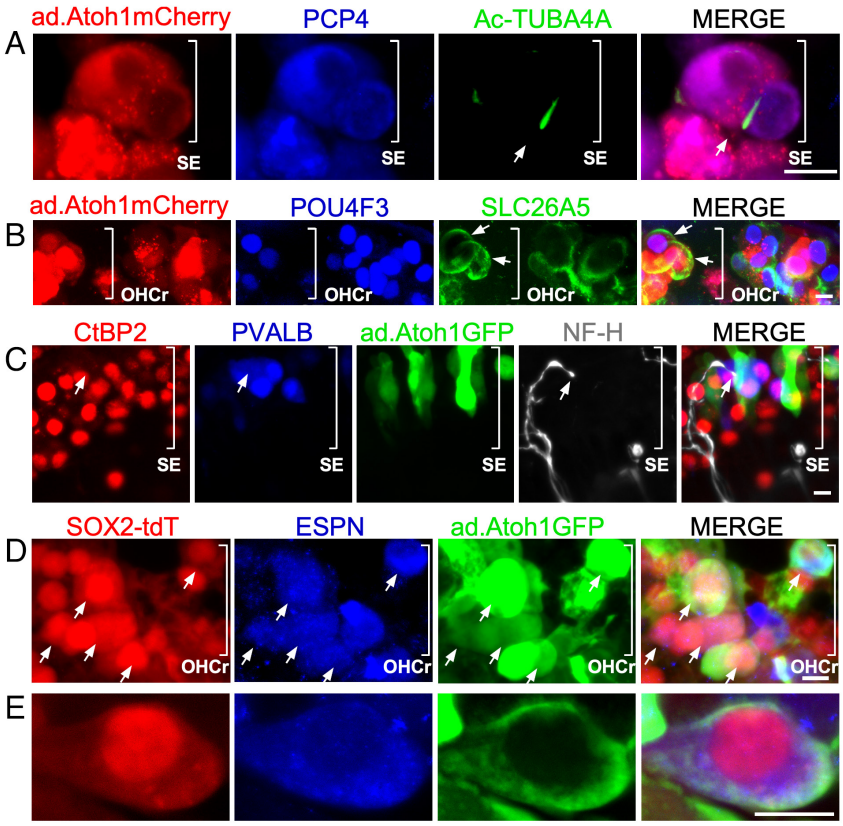

Fig. 5. Characteristics of regenerated HC-like cells. (*A*) Kinocilia labeled with acetylated tubulin (Ac-TUBA4A) in WT cochlea reprogrammed by the cocktail and infected by ad.*Atoh1.mCherry*. (*B*) SLC26A5 (prestin) positive HC-like cells (arrows) in WT cochlea treated with the cocktail and ad.*Atoh1.mCherry*. (*C*) The ganglion neurites (labeled with NF-H) were in contact with the immature synaptic ribbons in regenerated HC-like cell (Atoh1-GFP$^+$/PVALB$^+$). (*D* and *E*) Low and high magnification pictures delineating the in vivo lineage tracing result. The Tamoxifen-treated adult Sox2-tdTomato mice (4-wk-old) were i.p. injected with Kanamycin/Furosemide (Kana/Furo) to kill hair cells for 7 d, with the subsequent delivery of the cocktail (VLFsiFsiM) into the middle ear space, followed by the injection of Ad.*Atoh1-GFP* into the inner ear by cochleostomy for 21 d. In the reprogrammed mice, Ad.*Atoh1-GFP*-treated adult cochleae showed that most regenerated HC-like cells were of SC origin (arrows, ESPN$^+$/GFP$^+$/Sox2-tdT$^+$) in the outer hair cell region (OHCr) from the apex to the midturn. SE: sensory epithelial region.

of kinocilia. Again, we found Ac-TUBA4A$^+$ HC-like cells (11.5% ± 1.83%, mean ± SEM, n = 5 biological independent samples) in the Cocktail/ad-*Atoh1.mCherry*-treated WT cochlea explant culture (Fig. 5*A*). Auditory HCs can be divided into two specialized groups with distinct functions: OHCs and IHCs. Cochlear OHCs can be characterized by their expression of OHC marker prestin (SLC26A5). We detected SLC26A5$^+$/POU4F3$^+$/Atoh1-mCherry$^+$ in some regenerated HC-like cells (10.36% ± 2%, mean ± SEM, n = 6 biological independent samples), indicating a portion of regenerated HC-like cells start to express a marker for specialized auditory outer HCs (Fig. 5*B*). To study potential connection formed between regenerated HC-like cells and ganglion neurons, we performed CtBP2/NF-H/PVALB/Atoh1-*GFP* quad labeling. We found outgrowth of neurite (NF-H) to the sensory epithelial region to likely form contact with regenerated HC-like cell (Fig. 5*C*), whereas the overexpression of *Atoh1* or cocktail treatment itself neither regenerated POU4F3$^+$/MYO7A$^+$ HC-like cell nor preserved existing HCs (*SI Appendix*, Fig. S9 *E–H*). Taken together, we demonstrated that the novel "VLFsiFsiM cocktail" is sufficient to reprogram the adult mouse cochlea in lieu of MYC/NICD transgenes and regenerate HC-like cells in combination with *Atoh1* in vitro.

HC Regeneration by the VLFsiFsiM Cocktail in a Mouse Model with HC Loss In Vivo. Given the effect of the cocktail in reprogramming adult cochlea for HC-like cell regeneration in vitro, we sought to determine the effect on HC-like cell regeneration in adult WT mice in vivo. The composition of the cocktail of small molecules and siRNAs made it possible by middle ear delivery to achieve reprogramming. To study middle ear delivery, we first tested by injecting the cocktail VLFsiFsiM into the middle ear space in adult WT mice and collected the cochlea 4 d later to study the reprogramming effect. qPCR showed the upregulation of *Myc, Notch1,* and inner ear progenitor markers by the cocktail (*SI Appendix*, Fig. S8 *C* and *D*), indicating a similar reprogramming effect achieved in vivo by middle ear delivery. To determine whether the cocktail is sufficient for reprogramming for HC-like cell regeneration in vivo, we used a mouse model with severe HC loss induced by an ototoxic drug Kanamycin. We observed that, 7 d after intraperitoneal (i.p.) injection of Kanamycin and Furosemide, over 95% of OHCs were killed from apex-mid to middle turns, whereas the SCs (SOX2$^+$) were preserved in the same region, making it a good model to study HC regeneration in the OHC region in vivo (*SI Appendix*, Fig. S11 *A–C*). Using this HC damage model, we reprogrammed the damaged cochlea by injecting the VLFsiFsiM cocktail into the middle ear for 4 d, followed by injecting Ad.*Atoh1.mCherry* into the middle turn of the cochlea via cochleostomy (Fig. 6*A*). 21 d after Ad.*Atoh1.mCherry* injection, in control cochlea treated with vehicle (0.5% Dimethyl sulfoxide (DMSO)), occasional ESPN$^+$ HC-like cells were detected in the apex-mid that coincided with mCherry signals (Fig. 6*B*), an indication of regenerated HC-like cells. No HC-like cell was regenerated in the apex to mid-turn despite abundant infected SCs (Fig. 6*B* and *SI Appendix*, Fig S12*B*). In contrast, in the cochlea with cocktail treatment, numerous ESPN$^+$/mCherry$^+$ HC-like cells were seen from the apex to the mid-turn (Fig. 6*C*, *SI Appendix*, Fig. S12*C*, and Movies S1 and S2). Most regenerated HC-like cells were in the OHC region as the result of Ad.*Atoh1-mCherry* infection in SCs in the same region (Fig. 6*C* and *SI Appendix*, Fig. S12*C*). Compared to the control cochlea with OHC loss due to Kanamycin/Furosemide, there was a significant increase in the HC-like cell number in the OHC region in the cocktail-treated cochlea (Fig. 6 *D* and *F*). There was no change in the number of IHC due to the lack of Ad.*Atoh1-mCherry* infection in the region (Fig. 6*E*). Notably, many regenerated HC-like cells were positive for SOX2 (SOX2$^+$/ESPN$^+$, *SI Appendix*, Fig. S12*D*), indicating the transition from SCs to HC-like cells. Consistent with SC-to-HC transition, the total number of non-transdifferentiated SCs, i.e., SOX2$^+$/ESPN$^-$ SCs, was significantly reduced in the reprogramed

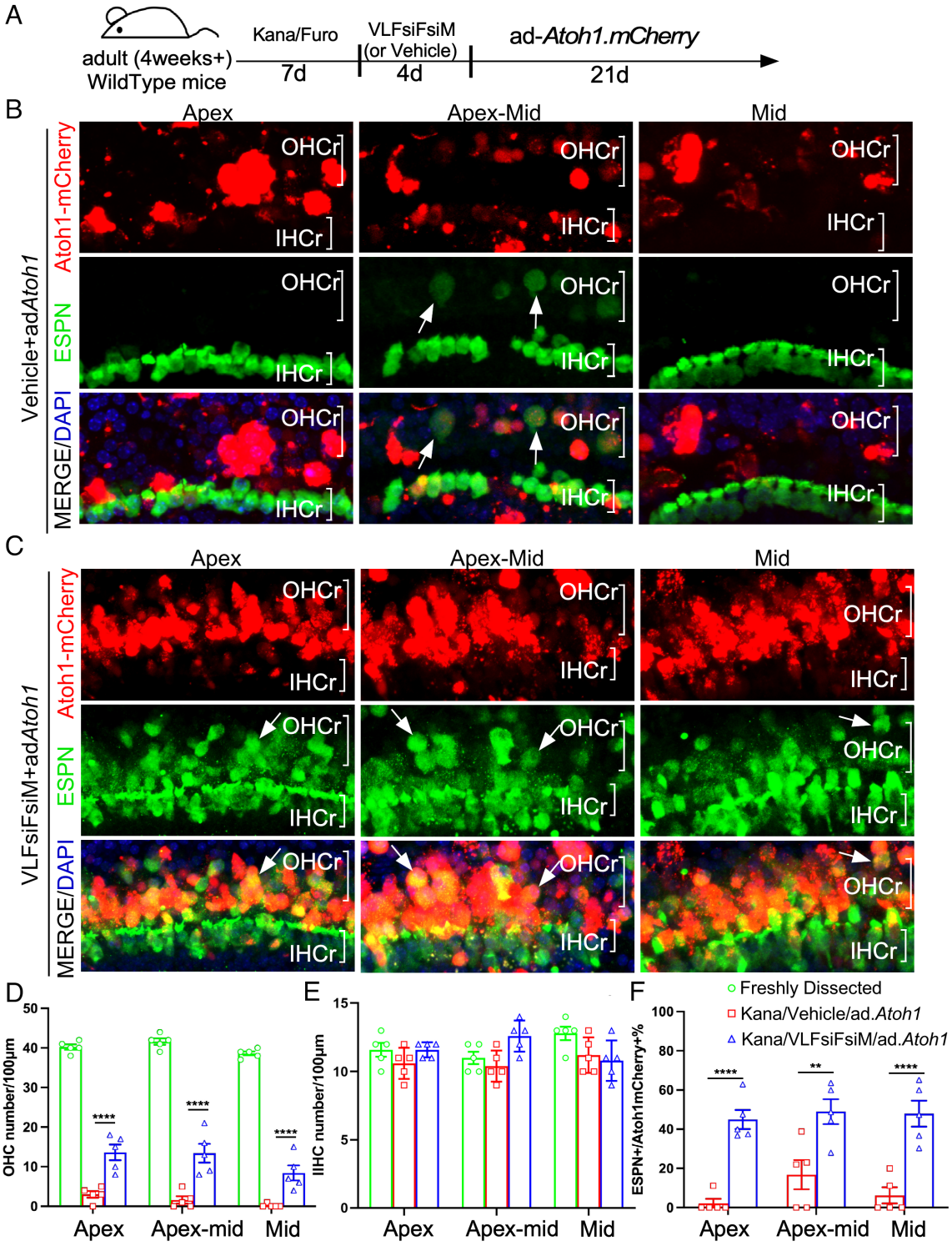

Fig. 6. Reprogramming and HC-like cell regeneration in a mouse model with HC loss in vivo. (*A*) A schematic diagram illustrating the experimental procedure that adult C57BL/6J mice were treated by Kanamycin/Furosemide (Kana/Furo) to kill hair cells, with the subsequent delivery of the cocktail (VLFsiFsiM) or vehicle (sterile water plus 0.1%DMSO) into the middle ear space, followed by the injection of Ad.*Atoh1.mCherry* into the inner ear by cochleostomy. (*B*) After Kana/Furo treatment, vehicles/Ad.*Atoh1-mCherry*-treated adult C57BL/6J cochleae showed scarce hair cells (arrows, ESPN$^+$/mCherry$^+$) in the outer hair cell region (OHCr) of the apex-middle turn. (*C*) After Kana/Furo treatment, cocktail/Ad.*Atoh1.mCherry*-treated adult C57BL/6j cochleae showed many hair cells (arrows, ESPN$^+$/mCherry$^+$) in the outer hair cell regions (OHCr) from the apex to the midturn. (*D*) Quantification and comparison of regenerated HC-like cells showed a significant increase in the HC-like cell number in the OHCr in the cocktail-treated samples compared to the vehicle-treated samples. (*E*) Quantification and comparison showed a comparable HC number in the IHC region in the cocktail-treated, vehicle-treated, and WT control cochlear samples. (*F*) Quantification and comparison showed significantly more ESPN+/Atoh1mCherry+ Cells in the cocktail-treated than vehicle-treated control cochlear samples. D: Dox; L: LiCl; F: FSK; siF: siFIR; siM: siMxi1. $^{**}P < 0.01$, $^{***}P < 0.001$, $^{****}P < 0.0001$, two-tailed unpaired Student's *t* test. Error bar, mean ± SEM; N = 5 to 6 in each group. Source data are provided as a Source Data file. (Scale bars, 10 μm.)

cochlea (*SI Appendix*, Fig. S12*E*), whereas the number of SCs in the IHC region remained constant (*SI Appendix*, Fig. S12*F*).

To further confirm SC-to-HC transdifferentiation, we performed in vivo lineage tracing study using the inducible *Sox2*-promoter-driven *Cre* mice (Sox2-CreER) cross with tdT reporter mouse, in which tamoxifen exposure activates tdT permanently and specifically in the SOX2$^+$ SC. With the same HC damage model, we reprogrammed the damaged cochlea by injecting the VLFsiFsiM cocktail into the

middle ear for 4 d, followed by injecting Ad.*Atoh1-GFP* into the middle turn of the cochlea via cochleostomy. The use of Ad.*Atoh1-GFP* was to circumvent the issue of Ad.*Atoh1.mCherry* that emitted the same wavelength color as the tdT. 21 d after Ad.*Atoh1-GFP* injection, numerous Sox2-tdT^{+}/ESPN^{+}/GFP^{+} HC-like cells were detected in the cocktail-treated WT adult cochlea (Fig. 5 *D* and *E*); Taken together, we demonstrated that the "VLFsiFsiM cocktail" delivered by middle ear is sufficient to reprogram WT adult mouse cochlea and regenerate HC-like cells in response to *Atoh1* in a severe HC loss mouse model in vivo.

Discussion

In this study, we used single-cell RNAseq to uncover the pathways underlying the MYC/NOTCH-mediated reprogramming of adult mouse cochlea. We further used the information to identify a combinatory approach by drug-like molecules to achieve reprogramming and HC-like cell regeneration in mature inner ear in vitro and in vivo (Fig. 7 for the summary).

Auditory inner ear HC regeneration in mature mammalian inner ear is a necessary step in order to develop a strategy to use HC regeneration to treat hearing loss. While most cochlear HC regeneration studies have focused on neonatal mice, recent studies by different groups including us have shown the feasibility of adult HC regeneration (8, 10, 13, 17, 18, 40–42). The regeneration efficiency in adult has been very low. We have developed a two-step approach to achieve auditory HC regeneration in the adult Organ of Corti: 1). Transient co-activation of cell cycle activator *Myc* and inner ear progenitor gene *Notch1* to reprogram adult cochlear SCs; 2). Overexpression of a transcription factor *Atoh1* in the reprogrammed SCs which then transdifferentiate into HC-like cells in vivo and in vitro (18).

For our ultimate goal to develop HC regeneration with clinical application, it is a prerequisite that *Myc/Notch* can be co-activated by drug-like molecules to achieve reprogramming in WT non-transgenic adult inner ear for efficient HC regeneration. To recapitulate the effect of MYC/NICD, we envisioned a replacement of MYC and NICD by drug-like small molecules and siRNAs. VPA is an established HDAC inhibitor and is a known Notch signal agonist (20, 21). Indeed, in the rtTA/tet-*Myc* mouse model, *Notch1* can be effectively activated with VPA (*SI Appendix*, Fig. S2*A*), which combined with Dox-induced MYC activation, results in efficient HC-like cell regeneration after Ad.*Atoh1* infection (Fig. 1 *B* and *C*), similar to what has been achieved by Dox induced reprogramming in the rtTA/tet-Myc/tet-NICD model (*SI Appendix*, Fig. S1). The result is consistent with the VPA-mediated *Notch1* activation, although other roles of VPA as an HDAC inhibitor in HC regeneration cannot be excluded.

Given that there is no known small molecule that can activate *Myc* potently, we first evaluated the possibility of using siRNAs to suppress *Myc* suppressors as a way to activate MYC. The siRNAs for *Fir* and *Mxi1*, two known MYC suppressors, exert a limited effect on MYC activation and HC-like cell regeneration (*SI Appendix*, Fig. S2*A*). However, the regeneration efficiency is much lower compared to what was achieved by MYC activation in the transgenic mouse model.

To compensate for the inefficient MYC activation by siRNAs, and to gain insight into the mechanisms underlying reprogramming in the adult cochlea, we sought to identify MYC/NICD downstream pathways in reprogramming by single-cell RNAseq using the rtTA/tet-*Myc*/tet-NICD model in which Dox activates MYC/NICD robustly. We hypothesized the analysis could provide a comprehensive view of the reprogramming pathways, which in turn could offer us the opportunity to manipulate some of them with drug-like molecules, to overcome the deficiency in MYC activation by siRNAs for efficient reprogramming and HC-like cell regeneration.

The RNAseq analysis identified nine transcriptionally distinct clusters of the major sensory epithelial cell types, most of which are characterized by the expression of marker genes (28–31). Few cell type clusters such as the pillar cells and phalangeal cells were not identified, which may be in part due to the effect of MYC/NICD that drastically altered the cell type identity. We used cultured adult cochleae for RNAseq, which may have some effect on cell type identity compared to acutely dissected cochleae. Another possibility is that after culture and dissociation, some cell types were lost disproportionately. Overall, the identification of most of the known cell types compared to freshly dissected cochlea from other studies (28, 30) and the presence of known marker gene expressions confirm the quality and comprehensiveness of our data.

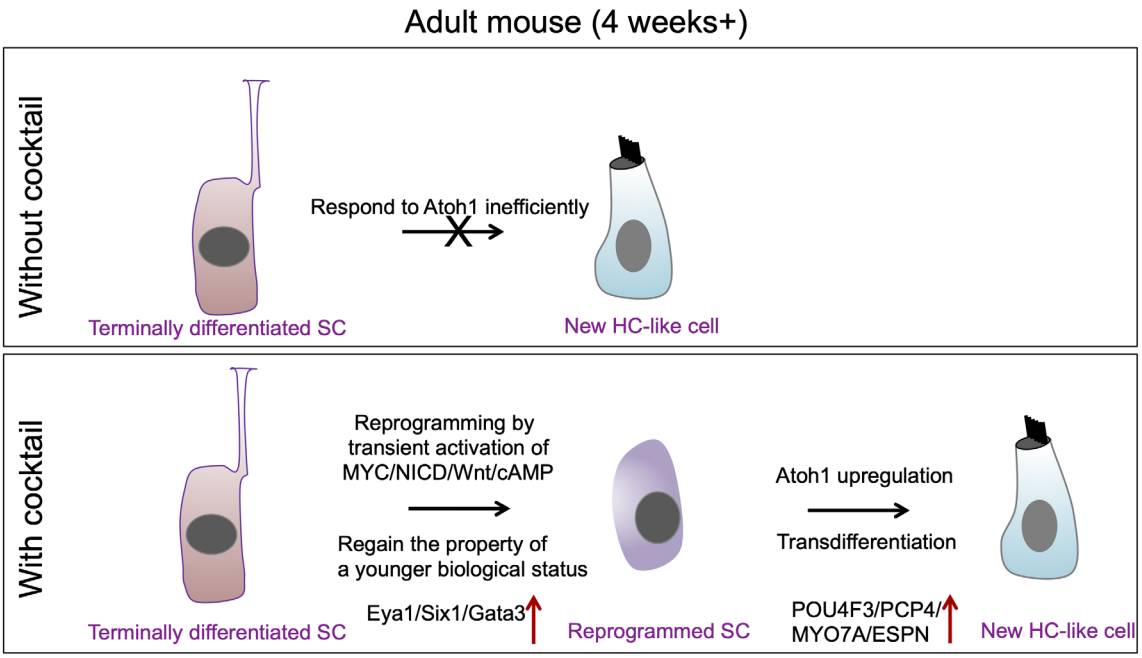

Fig. 7. A schematic diagram summarizing the working model for SC reprogramming by the drug-like molecules and HC-like cell regeneration.

The RNAseq data showed, following Dox-induced MYC/NICD activation, that the global transcriptional profiles of adult cochlear explants differed substantially from their control counterparts. The hallmark of MYC/NOTCH induced reprogramming is the heightened activities shown by genes in cell cycle and cell growth, which were enriched for genes involved in positive regulation of MYC target genes, E2F target genes, G2M cell cycle checkpoint genes, mitotic spindle genes, oxidative phosphorylation genes, MTORC1 and NOTCH signaling genes. A recent single-cell RNAseq study on zebrafish spontaneous HC regeneration after HC damage identified numerous pathways that are activated during different phases of reprogramming (43). Among the top identified pathways in zebrafish, many are shared with the reprogrammed adult mouse cochlea including the pathways in mitotic activities, oxidative phosphorylation, Notch and Wnt, supporting that those pathways are intrinsic to reprogramming and HC regeneration from zebrafish to mammals. However, some pathways we identified are unique to mouse, including cAMP, indicating the requirement of the pathways specifically for mammalian HC regeneration.

To gain insight into the transcriptional changes within cell types and to assess the origin of mitotically active cells in MYC/NICD-induced samples, we analyzed differential expression profiles of the highly represented MSigDB Hallmark genes across cell clusters. This analysis showed that distinct expression profiles for the Hallmark gene sets were more significantly enriched in the IdC populations, suggesting that MYC/NICD co-activation has a greater influence on the IdCs than on other inner ear cell types.

In our studies (*SI Appendix*, Fig. S1) (18), we noticed high-efficiency IdC to HC-like cell transdifferentiation in the limbus region, suggesting that the IdC may be under deeper reprogramming by MYC/NICD, which renders them more responsive to HC induction signals. This observation is consistent with the highly represented Hallmark gene sets in the IdC cluster by RNAseq. To characterize transcriptional events that are fundamental in IdC reprogramming, we utilized a pseudotime trajectory that allows for the construction of the co-regulated transcriptional networks during the transition between cell types and/or developmental stages. We identified four transcriptionally distinct subgroups of adult IdCs, depicted as transition stages from naive IdCs (Module #1) to the reprogrammed state (Module #4) (Fig. 3 *B* and *C*). The GO analysis of Module #4, the reprogrammed state, identified Wnt and Response to cAMP as two enriched signaling pathways, suggesting their involvement in MYC/NICD-mediated reprogramming. By qPCR, we confirmed the expression kinetics for the critical Wnt and cAMP-related genes across pseudo-time differentiation states of IdCs (*SI Appendix*, Fig. S7*B*). By the blockade of Wnt and cAMP pathways via small molecule inhibitors, cochlear HC-like cell regeneration is greatly attenuated despite MYC/NICD activation, demonstrating that Wnt and cAMP are downstream of MYC/NICD and are necessary for HC-like cell regeneration in the cultured adult cochlea (*SI Appendix*, Fig. S7). While the IdC cluster was used to identify the reprogramming pathways, blockade of the pathways led to a significant reduction in regenerated HC-like cells in the cochlear SE, which strongly supports the relevance of the IdC pathways in reprogramming the SE and HC regeneration. In addition to Wnt and cAMP, other pathways identified in the analysis can be studied in reprogramming and HC regeneration.

The discovery of Wnt and Response to cAMP pathways as downstream of MYC/NICD made it possible to activate both pathways by small molecules: Lithiumchloride (LiCl) to activate Wnt and FSK to activate cAMP. Wnt is a well-studied pathway in inner ear development and HC regeneration although its role in adult HC regeneration is not yet clear (44, 45). LiCl is a Wnt signaling agonist widely used in reprogramming terminally differentiated somatic cells into induced pluripotent stem cells (iPSCs) (46, 47). The application of LiCl causes the expansion of the prosensory domain with an increased number of HCs in the embryonic mouse cochlea (45). Interestingly, *Myc,* together with *Notch* in activating Wnt for reprogramming in the adult cochlea, is also a known downstream target of the Wnt signal pathway (48, 49). Clearly, there is a complex cross-talk between the pathways exerting the effect in both directions. cAMP was reported to be involved in the expansion of the auditory epithelium in both birds and mammals in the HC regeneration (50–52). FSK is the adenylate cAMP and has been utilized in replacing Yamanaka factors (YFs) in the protocol for chemical-iPSCs (53–55).

In our cocktail, we combined five components (VPA, LiCl, FSK and siRNA for Fir and Mxi1) to completely replace *Myc* and *Notch* transgenes to reprogram adult WT cochlea. We detected HC-like cell regeneration after Ad.*Atoh1* infection in vitro, with an efficiency that is similar to HC-like cell regeneration achieved in the rtTA/tet-*Myc*/tet-NICD mice, both of which are more efficient than that achieved by VPA/siF/siM, supporting additional reprogramming effect by LiCl and FSK. The study further highlights that the reprogramming pathways identified in the IdC cluster are directly relevant to HC regeneration in the cochlear SE. A combination of 13 chemicals has been shown to replace all four YFs to reprogram somatic cells into pluripotent stem cells (53), which is likely involved in deeper reprogramming. Our cocktail with five components likely results in partial reprogramming, to allow fully differentiated SCs to regain a relatively young-age status, which enables them to respond to *Atoh1* and transdifferentiate into HCs.

Excitingly, in the severe HC loss mouse model, new HC-like cells are regenerated from the "VLFsiFsiM" cocktail-treated reprogrammed SCs, compared to little HC-like cell regeneration in the vehicle-treated nonreprogrammed SCs. The data strongly support that chemical-mediated reprogramming and HC regeneration can be achieved in the mature mammalian cochlea. Our in vivo HC regeneration model by adenovirus infection directed the new HC-like cells to the right location of the $SOX2^+$ SE.

Despite the progress in our approach to achieve HC regeneration in the adult cochlea in vitro and in vivo, major challenges remain before potential clinical applications. First, regenerated HCs need to be terminally differentiated and fully mature, and to be located in the sensory epithelial region such that their stereocilia contact the tectorial membrane to mediate the mechanoelectrical transduction, as well as be able to survive long term. The current regenerated HC-like cells are immature and the time frame we used is not ideal to determine their long-term survival. One potential reason for the lack of terminal differentiation is the continuous *Atoh1* expression mediated by adenovirus, which is known to impact HC maturation and is detrimental to HC survival (9, 56). Future studies to express *Atoh1* transiently in the reprogrammed SCs could address the issue. Second, the surgical procedure of "cochleostomy" in the adult cochlea severely damages the microenvironment of the cochlea including extensive OHC death around the injection site. Future studies using an alternative delivery vehicle with a minimally invasive surgical procedure such as an AAV with round window injection could significantly improve HC regeneration efficiency without causing trauma to the inner ear. Third, major efforts should be made to identify/create new AAVs or novel delivery vehicles such as nanoparticles capable of targeting adult cochlear SCs for reprogramming. Finally, the restoration of hearing in adult deaf animal models significantly and reliably by HC regeneration will elevate the field of HC regeneration to a clinically relevant stage.

Our study provides an opportunity to achieve HC regeneration in the adult cochlea long after HC loss in WT mice in vivo. Given the drug-like properties of our cocktail in reprogramming, this work

strongly supports that the approach could be developed as a potential therapeutic method to regenerate HCs, with an important implication for the development toward future clinical applications.

Materials and Methods

Animals, Adult cochlear culture and viral infection in vitro, Single-cell preparation, Single-cell RNA library preparation and sequencing, Computational analysis of single-cell data, Single-cell trajectory analysis, pathway analysis, RNA-seq data availability, chemical reprogramming in vitro for HC regeneration, lineage tracing, transtympanic Injection of chemicals in vivo, viral Injection in vivo, immunohistochemistry, SEM, qRT-PCR, FM1-43 uptake and statistical analysis are described in *SI Appendix*.

Data, Materials, and Software Availability. All study data are included in the article and/or *SI Appendix*.

ACKNOWLEDGMENTS. We acknowledge funding from NIH R01DC006908, R01DC016875, R56DC006908, UG3TR002636 (Z.-Y.C.), The United State Department of Defense (DOD) W81XWH1810331 and W81XWH2110957 (Z.-Y.C.), Fredrick and Ines Yeatts HC regeneration fellowship (Z.-Y.C.), Harvard Catalysts Translational Innovator Program "The Five Senses" (Z.-Y.C.), NIH R01DC017166 and NIH R01DC020190 (A.A.I.), and Mike Toth Head and Neck Cancer center funds (S.V.S.). We thank Rozenn Riou in helping with operating Chromium Controller (S.V.S. Lab). We thank Stewart C. Silver for editing the manuscript.

Author affiliations: [a]Department of Otolaryngology-Head and Neck Surgery, Graduate Program in Speech and Hearing Bioscience and Technology, Harvard Medical School, Boston, MA 02115; [b]Department of Otolaryngology-Head and Neck Surgery, Graduate Program in Neuroscience, Harvard Medical School, Boston, MA 02115; [c]Eaton-Peabody Laboratory, Massachusetts Eye and Ear Infirmary, Boston, MA 02114; [d]Department of Otolaryngology-Head and Necks, Shengjing Hospital of China Medical University, Shenyang 110004, China; [e]Broad Institute of MIT and Harvard, Cambridge, MA 02142; and [f]Department of Otolaryngology Head and Neck Surgery, Massachusetts Eye and Ear Infirmary, Harvard Medical School, Boston, MA 02114

Author contributions: Y.-Z.Q., W.W., V.E., and Z.-Y.C. designed research; Y.-Z.Q., W.W., V.E., A.P.R., and C.T. performed research; Y.-Z.Q., W.W., V.E., S.V.S., and A.A.I. contributed new reagents/analytic tools; Y.-Z.Q., W.W., V.E., A.A.I., and Z.-Y.C. analyzed data; and Y.-Z.Q., W.W., V.E., M.H., and Z.-Y.C. wrote the paper.

1. J. T. Corwin, D. A. Cotanche, Regeneration of sensory hair cells after acoustic trauma. *Science* **240**, 1772–1774 (1988).
2. B. M. Ryals, E. W. Rubel, Hair cell regeneration after acoustic trauma in adult Coturnix quail. *Science* **240**, 1774–1776 (1988).
3. A. J. Hudspeth, How hearing happens. *Neuron* **19**, 947–950 (1997).
4. M. E. Warchol, P. R. Lambert, B. J. Goldstein, A. Forge, J. T. Corwin, Regenerative proliferation in inner ear sensory epithelia from adult guinea pigs and humans. *Science* **259**, 1619–1622 (1993).
5. A. Forge, L. Li, J. T. Corwin, G. Nevill, Ultrastructural evidence for hair cell regeneration in the mammalian inner ear. *Science* **259**, 1616–1619 (1993).
6. J. T. Corwin, Postembryonic production and aging in inner ear hair cells in sharks. *J. Comp. Neurol.* **201**, 541–553 (1981).
7. J. E. Jones, J. T. Corwin, Replacement of lateral line sensory organs during tail regeneration in salamanders: Identification of progenitor cells and analysis of leukocyte activity. *J. Neurosci.* **13**, 1022–1034 (1993).
8. J. L. Zheng, W. Q. Gao, Overexpression of Math1 induces robust production of extra hair cells in postnatal rat inner ears. *Nat. Neurosci.* **3**, 580–586 (2000).
9. Z. Liu *et al.*, Age-dependent in vivo conversion of mouse cochlear pillar and Deiters' cells to immature hair cells by Atoh1 ectopic expression. *J. Neurosci.* **32**, 6600–6610 (2012).
10. X. J. Li, C. Morgan, L. A. Goff, A. Doetzlhofer, Follistatin promotes LIN28B-mediated supporting cell reprogramming and hair cell regeneration in the murine cochlea. *Sci. Adv.* **8**, eabj7651 (2022).
11. Y. Chen *et al.*, Hedgehog signaling promotes the proliferation and subsequent hair cell formation of progenitor cells in the neonatal mouse cochlea. *Front. Mol. Neurosci.* **10**, 426 (2017).
12. N. Lu *et al.*, Sonic hedgehog initiates cochlear hair cell regeneration through downregulation of retinoblastoma protein. *Biochem. Biophys. Res. Commun.* **430**, 700–705 (2013).
13. J. Zhang *et al.*, ERBB2 signaling drives supporting cell proliferation in vitro and apparent supernumerary hair cell formation in vivo in the neonatal mouse cochlea. *Eur. J. Neurosci.* **48**, 3299–3316 (2018).
14. K. Kawamoto, S. Ishimoto, R. Minoda, D. E. Brough, Y. Raphael, Math1 gene transfer generates new cochlear hair cells in mature guinea pigs in vivo. *J. Neurosci.* **23**, 4395–4400 (2003).
15. M. Izumikawa *et al.*, Auditory hair cell replacement and hearing improvement by Atoh1 gene therapy in deaf mammals. *Nat. Med.* **11**, 271–276 (2005).
16. K. Mizutari *et al.*, Notch inhibition induces cochlear hair cell regeneration and recovery of hearing after acoustic trauma. *Neuron* **77**, 58–69 (2013).
17. B. J. Walters *et al.*, In vivo interplay between p27(Kip1), GATA3, ATOH1, and POU4F3 converts non-sensory cells to hair cells in adult mice. *Cell Rep.* **19**, 307–320 (2017).
18. Y. Shu *et al.*, Renewed proliferation in adult mouse cochlea and regeneration of hair cells. *Nat. Commun.* **10**, 5530 (2019).
19. C. Sage *et al.*, Essential role of retinoblastoma protein in mammalian hair cell development and hearing. *Proc. Natl. Acad. Sci. U.S.A.* **103**, 7345–7350 (2006).
20. D. Y. Greenblatt *et al.*, Valproic acid activates notch-1 signaling and regulates the neuroendocrine phenotype in carcinoid cancer cells. *Oncologist* **12**, 942–951 (2007).
21. X. Yin *et al.*, Niche-independent high-purity cultures of Lgr5+ intestinal stem cells and their progeny. *Nat. Methods* **11**, 106–112 (2014).
22. W. J. McLean *et al.*, Clonal expansion of Lgr5-positive cells from mammalian cochlea and high-purity generation of sensory hair cells. *Cell Rep.* **18**, 1917–1929 (2017).
23. W. Li *et al.*, A novel in vitro model delineating hair cell regeneration and neural reinnervation in adult mouse cochlea. *Front. Mol. Neurosci.* **14**, 757831 (2021).
24. A. Zine, R. Romand, Development of the auditory receptors of the rat: A SEM study. *Brain Res.* **721**, 49–58 (1996).
25. N. Schreiber-Agus *et al.*, An amino-terminal domain of Mxi1 mediates anti-Myc oncogenic activity and interacts with a homolog of the yeast transcriptional repressor SIN3. *Cell* **80**, 777–786 (1995).
26. K. Matsushita *et al.*, An essential role of alternative splicing of c-myc suppressor FUSE-binding protein-interacting repressor in carcinogenesis. *Cancer Res.* **66**, 1409–1417 (2006).
27. T. Stuart *et al.*, Comprehensive integration of single-cell data. *Cell* **177**, 1888–1902.e1821 (2019).
28. J. C. Burns, M. C. Kelly, M. Hoa, R. J. Morell, M. W. Kelley, Single-cell RNA-Seq resolves cellular complexity in sensory organs from the neonatal inner ear. *Nat. Commun.* **6**, 8557 (2015).
29. M. Hoa *et al.*, Characterizing adult cochlear supporting cell transcriptional diversity using single-cell RNA-seq: Validation in the adult mouse and translational implications for the adult human cochlea. *Front. Mol. Neurosci.* **13**, 13 (2020).
30. L. Kolla *et al.*, Characterization of the development of the mouse cochlear epithelium at the single cell level. *Nat. Commun.* **11**, 2389 (2020).
31. P. T. Ranum *et al.*, Insights into the biology of hearing and deafness revealed by single-cell RNA sequencing. *Cell Rep.* **26**, 3160–3171.e3163 (2019).
32. K. S. Yu *et al.*, Development of the mouse and human cochlea at single cell resolution. bioRxiv [Preprint] (2019). https://doi.org/10.1101/739680 (Accessed 30 June 2020).
33. A. Liberzon *et al.*, Molecular signatures database (MSigDB) 3.0. *Bioinformatics* **27**, 1739–1740 (2011).
34. A. Subramanian *et al.*, Gene set enrichment analysis: A knowledge-based approach for interpreting genome-wide expression profiles. *Proc. Natl. Acad. Sci. U.S.A.* **102**, 15545–15550 (2005).
35. W. Huang da, B. T. Sherman, R. A. Lempicki, Systematic and integrative analysis of large gene lists using DAVID bioinformatics resources. *Nat. Protoc.* **4**, 44–57 (2009).
36. W. Huang da, B. T. Sherman, R. A. Lempicki, Bioinformatics enrichment tools: Paths toward the comprehensive functional analysis of large gene lists. *Nucleic Acids Res.* **37**, 1–13 (2009).
37. D. Szklarczyk *et al.*, STRING v11: Protein-protein association networks with increased coverage, supporting functional discovery in genome-wide experimental datasets. *Nucleic Acids Res.* **47**, D607–D613 (2019).
38. J. M. Muncie *et al.*, Mechanical tension promotes formation of gastrulation-like nodes and patterns mesoderm specification in human embryonic stem cells. *Dev. Cell* **55**, 679–694.e611 (2020).
39. S. Kleinboelting *et al.*, Bithionol potently inhibits human soluble adenylyl cyclase through binding to the allosteric activator site. *J. Biol. Chem.* **291**, 9776–9784 (2016).
40. C. Sage *et al.*, Proliferation of functional hair cells in vivo in the absence of the retinoblastoma protein. *Science* **307**, 1114–1118 (2005).
41. P. M. White, A. Doetzlhofer, Y. S. Lee, A. K. Groves, N. Segil, Mammalian cochlear supporting cells can divide and trans-differentiate into hair cells. *Nature* **441**, 984–987 (2006).
42. C. Woods, M. Montcouquiol, M. W. Kelley, Math1 regulates development of the sensory epithelium in the mammalian cochlea. *Nat. Neurosci.* **7**, 1310–1318 (2004).
43. S. Baek *et al.*, Single-cell transcriptome analysis reveals three sequential phases of gene expression during zebrafish sensory hair cell regeneration. *Dev. Cell* **57**, 799–819.e796 (2022).
44. W. Li *et al.*, Notch inhibition induces mitotically generated hair cells in mammalian cochleae via activating the Wnt pathway. *Proc. Natl. Acad. Sci. U.S.A.* **112**, 166–171 (2015).
45. B. E. Jacques *et al.*, A dual function for canonical Wnt/beta-catenin signaling in the developing mammalian cochlea. *Development* **139**, 4395–4404 (2012).
46. Q. Wang *et al.*, Lithium, an anti-psychotic drug, greatly enhances the generation of induced pluripotent stem cells. *Cell Res.* **21**, 1424–1435 (2011).
47. K. Li *et al.*, Small molecules facilitate the reprogramming of mouse fibroblasts into pancreatic lineages. *Cell Stem. Cell* **14**, 228–236 (2014).
48. V. Muncan *et al.*, Rapid loss of intestinal crypts upon conditional deletion of the Wnt/Tcf-4 target gene c-Myc. *Mol. Cell Biol.* **26**, 8418–8426 (2006).
49. W. Shu *et al.*, Wnt/beta-catenin signaling acts upstream of N-myc, BMP4, and FGF signaling to regulate proximal-distal patterning in the lung. *Dev. Biol.* **283**, 226–239 (2005).
50. T. J. Bell, J. C. Oberholtzer, cAMP-induced auditory supporting cell proliferation is mediated by ERK MAPK signaling pathway. *J. Assoc. Res. Otolaryngol.* **11**, 173–185 (2010).
51. D. S. Navaratnam, H. S. Su, S. P. Scott, J. C. Oberholtzer, Proliferation in the auditory receptor epithelium mediated by a cyclic AMP-dependent signaling pathway. *Nat. Med.* **2**, 1136–1139 (1996).
52. M. Montcouquiol, J. T. Corwin, Brief treatments with forskolin enhance s-phase entry in balance epithelia from the ears of rats. *J. Neurosci.* **21**, 974–982 (2001).
53. S. Cao *et al.*, Chromatin accessibility dynamics during chemical induction of pluripotency. *Cell Stem. Cell* **22**, 529–542.e525 (2018).
54. P. Hou *et al.*, Pluripotent stem cells induced from mouse somatic cells by small-molecule compounds. *Science* **341**, 651–654 (2013).
55. Y. Post *et al.*, Snake venom gland organoids. *Cell* **180**, 233–247.e221 (2020).
56. Z. Liu, J. Fang, J. Dearman, L. Zhang, J. Zuo, In vivo generation of immature inner hair cells in neonatal mouse cochleae by ectopic Atoh1 expression. *PLoS One* **9**, e89377 (2014).